AQP5 is Differentially Regulated in Astrocytes During Metabolic and Traumatic Injuries

Rui Chao Chai,[1,2] Jiao Hua Jiang,[1,2] Ann Yuen Kwan Wong,[1,2] Feng Jiang,[1,2] Kai Gao,[1,2] Greg Vatcher,[1,2] and Albert Cheung Hoi Yu[1,2,3]

Water movement plays vital roles in both physiological and pathological conditions in the brain. Astrocytes are responsible for regulating this water movement and are the major contributors to brain edema in pathological conditions. Aquaporins (AQPs) in astrocytes play critical roles in the regulation of water movement in the brain. AQP1, 3, 4, 5, 8, and 9 have been reported in the brain. Compared with AQP1, 4, and 9, AQP3, 5, and 8 are less studied. Among the lesser known AQPs, AQP5, which has multiple functions identified outside the central nervous system, is also indicated to be involved in hypoxia injury in astrocytes. In our study, AQP5 expression could be detected both in primary cultures of astrocytes and neurons, and AQP5 expression in astrocytes was confirmed in 1- to 4-week old primary cultures of astrocytes. AQP5 was localized on the cytoplasmic membrane and in the cytoplasm of astrocytes. AQP5 expression was downregulated during ischemia treatment and upregulated after scratch-wound injury, which was also confirmed in a middle cerebral artery occlusion model and a stab-wound injury model *in vivo*. The AQP5 increased after scratch injury was polarized to the migrating processes and cytoplasmic membrane of astrocytes in the leading edge of the scratch-wound, and AQP5 over-expression facilitated astrocyte process elongation after scratch injury. Taken together, these results indicate that AQP5 might be an important water channel in astrocytes that is differentially expressed during various brain injuries.

GLIA 2013;61:1748–1765

Key words: aquaporin, ischemia, MCAO, scratch-wound, stab-wound

Introduction

Aquaporins (AQPs) are a family of channel proteins which facilitate the rapid transport of water and solutes across membranes (Agre, 2006; Preston and Agre, 1991; Preston et al., 1992). Water movement in the brain, in which AQPs play a major role, is of great physiological and pathological importance, as about 80% of the content of the brain is water (Tait et al., 2008). Neuronal activity is accomplished by water and ion movement across membranes, while brain edema, or swelling, which is a result of a water homeostasis disorder, is a life threatening side effect of many brain injuries and diseases (Badaut et al., 2002). Astrocytes are the most numerous cells in the brain and play a critical role in the maintenance of water homeostasis, and astrocytes show the most prominent swelling of all cell types during brain edema under pathological conditions in the central nervous system (CNS) (Albertini and Bianchi, 2010; Tait et al., 2008). Clarifying the expression, localization and functions of AQPs in astrocytes is critical to understand the complicated water flux in the CNS.

AQP1, 3, 4, 5, 8, and 9 have been reported to be expressed in the brain (Badaut et al., 2002; Yamamoto et al., 2001). AQP1, 4, and 9 serve multiple functions, including regulation of water movement, regulation of astrocyte volume

View this article online at wileyonlinelibrary.com. DOI: 10.1002/glia.22555

Published online Aug 6, 2013 in Wiley Online Library (wileyonlinelibrary.com). Received Feb 8, 2013, Accepted for publication June 17, 2013.

Address correspondence to Albert Cheung Hoi Yu, Neuroscience Research Institute, Peking University, 38 Xue Yuan Road, Beijing 100191, China. E-mail: achy@hsc.pku.edu.cn

From the [1]Neuroscience Research Institute & Department of Neurobiology, School of Basic Medical Sciences, Peking University, Beijing 100191, China; [2]Key Laboratory for Neuroscience, Ministry of Education/National Health and Family Planning Commission, Peking University, Beijing 100191, China; [3]Laboratory of Translational Medicine, Institute of Systems Biomedicine, Peking University, Beijing 100191, China.

Additional Supporting Information may be found in the online version of this article

changes, facilitation of reactive astrocyte migration, and production of cerebrospinal fluid (Badaut et al., 2002; Badaut and Regli, 2004; Bondy et al., 1993; Manley et al., 2000; Papadopoulos and Verkman, 2013; Rash et al., 1998; Strange, 1992; Yool, 2007). However, the functions of AQP3, 5, and 8 are still unclear. AQP4 is the most studied AQP in astrocytes and is mainly localized on the cytoplasmic membrane and end feet, where it plays a crucial role in regulating water flow into and out of the brain. AQP4 is also involved in brain edema caused by ischemia and other injuries, and the reactive astrocyte migration and glial scar formation that occurs after traumatic brain injuries (Manley et al., 2000; Meng et al., 2004; Papadopoulos et al., 2004; Saadoun et al., 2005; Sun et al., 2003; Zador et al., 2009). However, AQP4-null mice have normal brain vascular anatomy and morphology, and normal astrocytic proliferation and adhesion functions (Manley et al., 2000; Papadopoulos and Verkman, 2013; Saadoun et al., 2005). The speed of cell migration in AQP4-null mouse astrocytes was only reduced by 34.2% after scratch injury (Saadoun et al., 2005), and the cellular volumes of both $AQP4^{(-/-)}$ and $AQP4^{(+/+)}$ astrocytes were significantly increased after hypoxia injury (Fu et al., 2007). All these facts suggest that there might be other AQPs in astrocytes that compensate for the loss of AQP4. AQP1 and AQP9 expression in astrocytes is also upregulated after traumatic brain injury (McCoy and Sontheimer, 2010). AQP5 mRNA is downregulated after hypoxia injury (Yamamoto et al., 2001), indicating that AQP5 may be another important water channel in astrocytes, in addition to AQP1, 4, and 9.

AQP5 is expressed on the membranes of epithelial cells in corneal, pancreatic, and bronchial epithelium, the secretory cells in salivary and lacrimal glands, airway submucosal glands, and Type I pneumocytes of the respiratory tract (Sidhaye et al., 2012). Some of the known functions of AQP5 include: conveying a high degree of membrane water permeability (King et al., 2004; Krane et al., 2001; Ma et al., 1999), regulating water movement through the paracellular pathway (Kawedia et al., 2007; Sidhaye et al., 2008), gas permeability (Musa-Aziz et al., 2009), and cell cytoskeleton regulation (Sidhaye et al., 2008, 2012). Recently, AQP5 has been considered as a marker protein for cell proliferation and migration in breast cancer and plays an important role in facilitating tumor metastasis (Jung et al., 2011; Shi et al., 2012; Zhang et al., 2010). AQP5 is expressed in several common human glioma cell lines and acute patient biopsies (McCoy and Sontheimer, 2007). However, compared with the well-understood water channels in the brain, such as AQP1, 4, and 9 (Papadopoulos and Verkman, 2013), less is known about AQP5. The fact that the expression of AQPs is differentially regulated during different brain injuries also suggests that AQPs are important factors involved in brain dysfunction. For example, AQP4 expression fluctuates in astrocytes during brain edema (Tait et al., 2008) and is differentially regulated in different injuries, such as brain ischemia and traumatic brain injury (Meng et al., 2004; Sun et al., 2003). Clarifying the expression of AQP5 during different injuries in astrocytes is a first step towards understanding the roles of AQP5 in astrocytes under physiological and pathological conditions.

In this study, we confirmed that AQP5 was expressed in both mouse primary cultures of astrocytes and rat brain. AQP5 was also differentially expressed in ischemic and traumatic injuries, in both *in vitro* and *in vivo* models. These results indicated that AQP5 might be another important water channel in astrocytes, in addition to AQP1, 4, and 9, which facilitates astrocytic responses to different injuries.

Materials and Methods

Primary Cultures of Cerebral Cortical Astrocytes and Neurons

Primary cultures of cerebral cortical astrocytes were prepared, as previously described (Dong et al., 2009; Yang et al., 2011; Yu et al., 2001; Zhou et al., 2010), from newborn (within 24 h after birth) ICR mice. Briefly, meninges-free cerebral cortices were cut into small cubes and suspended in modified Dulbecco's Modified Eagle's Medium (DMEM). After mechanical dissociation, the cell suspension was sequentially passed through 70 μm and 10 μm nylon filters (Spectra/Mesh, Spectrum Medical Industries). 10% (v/v) fetal bovine serum (FBS; Hyclone, Australia) was added to the medium containing filtered cell suspensions. Cells were seeded in 35 mm tissue culture dishes (Corning) at 3.5×10^5 cell/mL. Cultures were then incubated at 37°C, with 95% air/5% CO_2 (v/v) and 95% humidity. Culture medium was changed twice per week with DMEM containing 10% (v/v) FBS for the first 2 weeks and 7% (v/v) FBS afterward. Astrocytes were used for experiments after 4 weeks.

Primary cultures of cortical neurons were prepared from embryonic ICR mice (Day 16) as previously described (Zhou et al., 2010). In brief, meninges-free cerebral cortices were cut into small pieces and digested with 0.25% trypsin. Cells were suspended in modified DMEM and passed through a 70 μm nylon filter. Cells were grown in modified DMEM with 5% horse serum (Hyclone, Australia) in 35 mm tissue culture dishes (Corning) precoated with poly-D-lysine (25 μg/mL, Sigma-Aldrich) overnight. Cytosine arabinoside (40 μM; Sigma-Aldrich) was added on Day 3 to inhibit the growth of astrocytes. Neurons were used for experiments on Day 7.

Reverse Transcription Polymerase Chain Reaction and Real-Time Polymerase Chain Reaction

Gene expression of AQPs in mouse tissues, astrocytes, and neurons was measured with reverse transcription polymerase chain reaction (RT-PCR). Total RNA from mouse tissues and cultured cells was extracted using TRIzol reagent (Invitrogen) according to the manufacturer's instructions. 1 μg of total RNA was used as template for reverse transcription (RT). PCR (with 30 cycles of 94°C, 30 s;

65°C, 30 s; 72°C, 30 s; and a final extension at 72°C for 10 min) was performed using 2 μL of cDNA in a total volume of 20 μL. GAPDH was used as an internal control. AQP5 mRNA expression in astrocytes with ischemia treatment or scratch treatment was measured with real-time PCR. cDNA and GoTaq® qPCR Master Mix (Promega) were used to perform the real-time PCR according to the standard procedure instructions with an ABI Prism 7500 real-time PCR system (Applied Biosystems). GAPDH was also used as an internal control. Primers used for amplifying the AQP genes and GAPDH were based on sequences of murine AQP isoforms and GAPDH retrieved from the PubMed database (http://www.ncbi.nlm.nih.gov/pubmed). The sequences of primers used in RT-PCR were as follows: for AQP1: forward: 5′-GGC CAT GAC CCT CTT CGT CTT CA-3′; reverse: 5′-AGG TCA TTG CGG CCA AGT GAA TT-3′. For AQP4: forward: 5′-CTG GAG CCA GCA TGA ATC CAG-3′; reverse: 5′-TTC TTC TCT TCT CCA CGG TCA-3′. For AQP5: forward: 5′-CTC TGC ATC TTC TCC TCC ACG-3′; reverse: 5′-TCC TCT CTA TGA TCT TCC CAG-3′. For AQP7: forward: 5′-GAG TCG CTA GGC ATG AAC TCC-3′; reverse: 5′-AGA GGC ACA GAG CCA CTT ATG-3′. For AQP9: forward: 5′-CCT TCT GAG AAG GAC CGA GCC-3′; reverse: 5′-CTT GAA CCA CTC CAT CCT TCC-3′. For GAPDH: forward: 5′-TCA CCA CCA TGG AGA AGG C-3′; reverse: 5′-GCT AAG CAG TTG GTG GTG CA-3′. PCR products were separated on 2% agarose gels with ethidium bromide and photographed under an ultraviolet illuminator.

Ischemia Treatment

Ischemia treatment was performed as previously described (Chen et al., 2005; Dong et al., 2009; Lau and Yu, 2001; Yu et al., 2001; Zhou et al., 2010). The medium used in ischemia experiments was glucose and serum-free modified DMEM, and was equilibrated with anaerobic gas (85% N_2, 10% H_2, 5% CO_2), the treatment was performed in an anaerobic chamber (85% N_2, 10% H_2, 5% CO_2, 37°C; Forma Scientific). Astrocytes were washed twice with ischemic medium, and then incubated with 0.8 mL ischemic medium per 35 mm culture dish for 0, 0.5, 2, 4, and 6 h.

Middle Cerebral Artery Occlusion

All animal studies were approved by the Institutional Animal Care and Use Committee of Peking University. Middle cerebral artery occlusion (MCAO) was performed as reported (Guo et al., 2012; Hu et al., 2011; Shi et al., 2012). Briefly, adult male Sprague–Dawley (SD) rats (280 g to 320 g) were anesthetized with 4% isoflurane and maintained with 2.0% isoflurane, 30% oxygen, and 70% air. The right common carotid artery was exposed, and the internal carotid artery was ligated, then the external carotid artery was divided with a stump of 3–4 mm. The stump of the external carotid artery was opened, a 4.0 monofilament nylon suture was inserted up to 18–20 mm, or until resistance was felt, through the internal carotid artery. After occlusion for 2 h, the suture was withdrawn. The heart rate and blood glucose levels before, during, and after ischemia were monitored. After reperfusion for the designated time, rats were then perfused through the heart with phosphate-buffered saline (PBS) to remove all blood, and fixed with 4% paraformaldehyde (PFA) after the suture was withdrawn. The brains were isolated from the rats and frozen until analyzed.

Scratch-Wound Injury Treatment

Scratch-wound injury experiments were performed as previously described (Lau and Yu, 2001; Yang et al., 2012; Yu et al., 1993). Cultures were scratched with a 200 μL sterile plastic pipette tip according to a grid. The scratch caused an average of 37% injury to the plated culture. The culture medium was changed immediately following the scratch-wound to remove most of the detached cells and debris, and then the cultures were incubated in fresh modified DMEM containing 10% FCS in an incubator (5% CO_2, 37°C).

Stab-Wound Injury

Stab-wound injury was performed as reported (Anderova et al., 2004; Koyama et al., 1999; Simon et al., 2011). Briefly, male Sprague Dawley rats (280 g–320 g) were anesthetized with chloral hydrate (0.4 g/kg, i.p.), and all the following operation procedures were performed on a stereotaxic apparatus (David Kopf Instruments). The scalp was incised, and a small slit made with a dental drill, and a number 23 dissection blade was inserted through the slit (3.8 mm right/left side, from 1.5 mm anterior to 1.5 mm posterior of the bregma, and 5.0 mm depth from surface of the skull). The rats, 7 days after stab-wound injury, were perfused through the heart with PBS, and then fixed with 4% PFA. The brains were isolated from the rats and frozen until analyzed.

Subcellular Fraction Preparation

The subcellular fractions were prepared according to the Abcam® protocol. Confluent astrocytes were washed three times with ice-cold PBS, then 200 μL of ice-cold fractionation buffer [0.25 M sucrose, 25 mM KCl, 10 mM $MgCl_2$, 20 mM HEPES (pH 7.4), 1 mM DTT, and 0.1 mM phenylmethylsulfonyl fluoride (PMSF)] was added to the 35 mm culture dishes, and the cell lysate was collected in a 1.5 mL Eppendorf tube on ice. The lysate was then passed through a 25 G needle 10 times with a 1 mL syringe, and incubated on ice for 15 min. Centrifugation at 720*g*, 4°C for 5 min produced the crude nuclear pellet (P1). The supernatant was transferred into a fresh tube, and then centrifuged again at 10,000*g*, 4°C for 10 min, the resulting supernatant contained the cytoplasm and membrane fraction (S1), while the pellet formed the crude mitochondria fraction (P2). The P1 was washed by adding another 200 μL of fractionation buffer, dispersed with a pipette, passed through a 25 G needle 10 times, and centrifuged at 1,000*g*, 4°C for 10 min, and the resulting pellet contained the nuclear fraction. To further separate the membrane fraction and cytosolic fraction, the S1 was centrifuged at 100,000*g*, 4°C for 1 h, the supernatant was the cytosolic fraction, and the pellet was the membrane fraction. The P2 was washed by adding another 200 μL of fractionation buffer, dispersed with a pipette, passed through a 25 G needle 10 times, and centrifuged at 10,000*g*, 4°C for 10 min, the pellet was the mitochondria fraction.

Western Blot Analysis

After washing with ice-cold PBS three times, cells or isolated cell fractions were lysed in ice-cold lysis buffer [150 mM NaCl, 0.1%

(w/v) NP-40, 50 mM Tris (pH 8.0), 0.5% (w/v) sodium deoxycholate, 1% (w/v) SDS, 1 mM DTT, 0.1 mM PMSF, and protease inhibitor cocktail (Roche, Sweden)]. A Lowry protein assay was used to measure the total protein content. The proteins were boiled and analyzed with a standard Western blot procedure. Briefly, proteins were electrophoresed on a 12% sodium dodecyl sulfate polyacrylamide gel electrophoresis (SDS-PAGE) gel, and were then electrophoretically transferred onto PVDF membranes (Millipore). The PVDF membranes were blocked with 5% (w/v) nonfat milk in TBST buffer [0.1 M Tris-HCl (pH 8.0), 0.9% (w/v) NaCl, and 0.1% (v/v) Tween-20], and the target proteins were probed with diluted primary antibodies to AQP5 (1:1,000; Santa Cruz), AQP1 (1:1,000; Abcam), AQP4 (1:1,000; Millipore), Lamin A (1:1,000; Santa Cruz), β-Tubulin (1:2,000; Cell Signaling Technology), COX4 (1:2,000; Abcam), or transferrin receptor (1:2,000; Abcam) in blocking solution overnight at 4°C. The membranes were then incubated with the second antibody conjugated with horse-radish peroxidase (1:2,000; Santa Cruz) for 1 h at room temperature. Finally, an enhanced chemiluminescent Western blot detection kit (Santa Cruz) was used to detect the expression of the target proteins.

Immunofluoresent Staining

Immunofluoresent staining was performed as previously described (Chen et al., 2005). Confluent astrocytes were washed three times with ice-cold PBS, fixed with 4% PFA for 20 min, and permeabilized with 0.3% Triton X100 for 15 min. The cultures were then blocked with 3% BSA in PBS for 30 min at room temperature and incubated with primary antibody (anti-AQP5 1:50, Santa Cruz; anti-GFAP 1:200, Santa Cruz; anti-AQP4 1:50, Millipore) at 4°C overnight. After washing three times with PBS, the cultures were incubated with secondary antibody conjugated with DyLight 488 or Cyanine Dye 3.5 or DyLight 594 (1:200, Invitrogen) for 1 h at room temperature. Hoechst 33342 (2 μg/mL, Sigma-Aldrich) was used to stain nuclei. Finally, the cultures were observed with a confocal microscope (Olympus, Japan). All the photographs shown in the results were representative photographs from at least three experiments.

Plasmid Construction

The AQP4-EGFP plasmid was a kind gift from K. Nakahama (Department of Anatomy, Kinki University School of Medicine, Osakasayama City, Osaka, Japan). For the construction of the AQP1-EGFP, AQP5-EGFP, and AQP9-EGFP, total RNA was extracted from astrocytes using TRIzol reagent and was reverse-transcribed using the Moloney Murine Leukemia Virus RT-PCR system (Promega) with random hexamer (Promega). The AQP1, 5, and 9 coding domain sequence without termination codon was inserted into the pEGFP-N1 or other vectors (Clontech). The constructed plasmids were sequenced to confirm the correct AQP1, 5, and 9 sequence as published in GenBank.

Transfection

For transfection of primary astrocytes cultured in 35-mm dishes, 2 μg of plasmid DNA and 2 μL of Lipofectamine® 2000 (Invitrogen) were used. Plasmid DNA and Lipofectamine® 2000 reagent were separately diluted in 0.05 mL DMEM for 5 min, then mixed and incubated for 30 min at room temperature. The DNA/Lipofectamine® 2000 mixture was then added to cells prewashed with DMEM and incubation continued for 6 h at 37°C with 95% air/5% CO_2 (v/v) and 95% humidity. Subsequently, medium was replaced by fresh DMEM supplemented with 10% (v/v) FBS. Transfected astrocytes were maintained for 48 to 72 h before further experimentation.

Statistical Analysis

Experiments were repeated at least three times with different batches of cultures in independent experiments. Results were analyzed using PRISM 5.0 software (GraphPad Software). Data was expressed in the form of mean ± S.E.M. Statistical analysis was performed using a Student's *t*-test or one-way analysis of variance (ANOVA) with Bonferroni post test for multiple comparisons. Results were considered as statistically significant when $P < 0.05$.

Results

AQP5 Expression in Brain Tissue and Primary Cultures of Astrocytes

The expression of AQP1, 4, 5, 7, and 9 in mouse brain cerebral cortex was examined by RT-PCR. The expressions of AQP1 and AQP7 in mouse kidney, as well as the expression of AQP5 in lung tissue, were used as positive controls. There were strong bands for AQP1 and AQP7 in the kidney samples, and a strong band for AQP5 in lung tissue. The mouse brain cerebral cortex samples showed positive bands for AQP1, 4, 5, and 9, but not for AQP7 (Fig. 1A). The results indicated that AQP5 was expressed in mouse cerebral cortex.

To examine the expression of AQP5 in astrocytes and neurons in mouse cerebral cortex, the mRNA levels of AQP4 and AQP5 in 4-week-old primary cultures of cerebral cortical astrocytes and in 1-week-old primary cultures of cerebral cortical neurons was measured by RT-PCR (Fig. 1B). The brain cerebral cortex and lung samples were used as positive controls for AQP4 and AQP5, respectively. In astrocyte samples, bands for both AQP4 and AQP5 were clearly observed. In neurons, a band for AQP5 was detected, while a weak band for AQP4 was also detected. These results indicated that AQP5 was expressed both in astrocytes and neurons.

The level of AQP4 and AQP5 mRNA in 1- to 4-week old primary cultures of astrocytes were measured by RT-PCR (Fig. 1C,D). Both AQP4 and AQP5 expression was detected in 1- to 4-week-old primary cultures of astrocytes, and the expression of AQP5 mRNA significantly increased in 2-week-old and 3-week-old primary cultures of astrocytes. AQP5 expression was also increased in 4-week-old primary cultures of astrocytes, but without a statistical difference when compared with 1-week-old primary cultures of astrocytes. AQP5 protein expression also increased similarly to the mRNA expression in 1- to 4-week-old primary cultures of astrocytes

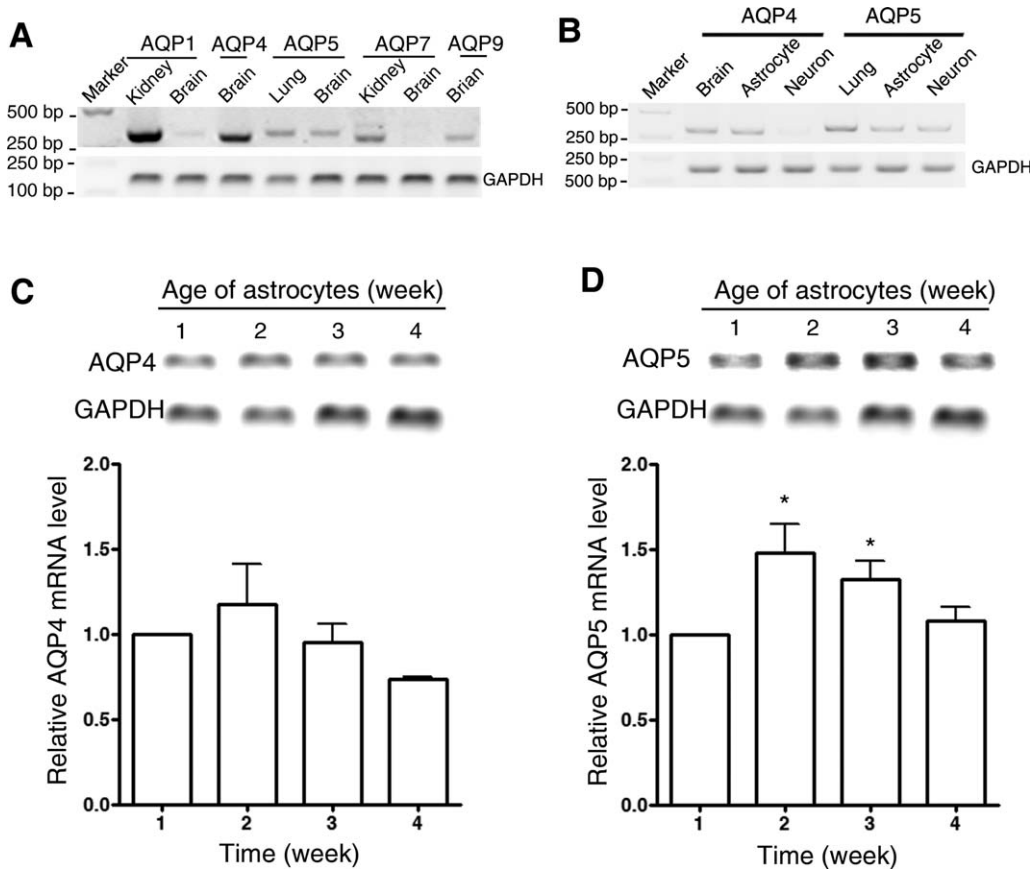

FIGURE 1: Expression of AQP5 in brain and primary cultures of astrocytes. (A) The expression of AQP mRNAs (AQP1, 4, 5, 7, and 9) were detected in the brain tissue of ICR mice with reverse transcription PCR (RT-PCR), mouse kidney was used as positive control for AQP1 and AQP7, and mouse lung for AQP5. GAPDH was used as internal control. (B) The expression of AQP4 and AQP5 mRNA was detected in primary cultures of astrocytes and neurons. Positive controls for AQP4 and AQP5 were brain tissue and kidney tissue, respectively. GAPDH was used as internal control. (C) The mRNA level of AQP4 in primary cultures of astrocytes of different ages was measured with RT-PCR. The mRNA of AQP4 was detected in 1-, 2-, 3-, and 4-week-old primary cultures of astrocytes. GAPDH was used as internal control. The bottom panel is a quantification of the mRNA level of AQP4 in 1-, 2-, 3-, and 4-week-old primary cultures of astrocytes. $n = 3$ from three different experiments. (D) The mRNA level of AQP5 in primary cultures of astrocytes of different ages was measured by RT-PCR. The mRNA of AQP5 was detected in 1-, 2-, 3-, and 4-week-old primary cultures of astrocytes. GAPDH was used as internal control. The bottom panel is a quantification of the mRNA level of AQP5 in differently-aged primary cultures of astrocytes. $n = 3$ from three different experiments. $^*P < 0.05$.

(Fig. 2). AQP5 protein was significantly increased in 2- to 4-week-old primary cultures of astrocytes compared with 1-week-old primary cultures. These results indicated that both AQP5 mRNA and protein were expressed in 1- to 4-week-old primary cultures of astrocytes, and that the expression was increased in 2- to 4-week-old cultures compared with 1-week-old cultures.

Subcellular Localization of AQP5 in Primary Cultures of Astrocytes

To confirm the specificity of the AQP5 antibody and study the localization of different AQPs in primary cultures of astrocytes, we performed AQP5 immunostaining with the AQP5 antibody in astrocytes transfected with AQP1, 4, 5, and 9-EGFP (Fig. 3). The results indicated that prominent increased AQP5 immunostaining signals could only be observed in AQP5-EGFP-positive astrocytes, and the immunostaining signals were co-localized with AQP5-EGFP signals, while AQP5 staining signals did not co-localize with AQP1, 4, or 9-EGFP signals in astrocytes. In addition, AQP5 immunostaining and AQP5-EGFP signals were observed in both the cytoplasm and cytoplasmic membrane. We also observed the AQP1, 4, and 5 protein expressions in astrocytes with a Western blot (Supp. Info. Fig. S1). In the three samples separated from the same astrocyte total cell lysate, all the bands (with different molecular weights) for AQP1, 4, and 5 proteins were detected.

To further elucidate the localization of AQP5 in primary cultures of astrocytes, we compared the localization of AQP5 and AQP4 in the same astrocytes (Fig. 4A,B). The results revealed that AQP5 localized to both the cytoplasm and the cytoplasmic membrane, while AQP4 mainly accumulated at the cytoplasmic membrane. This result was consistent

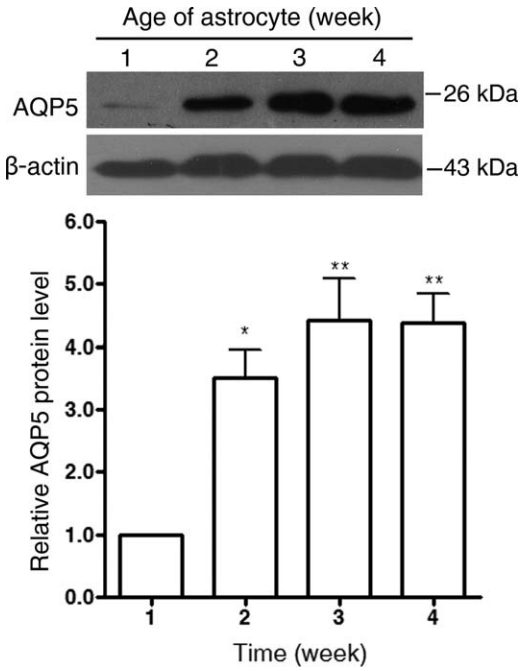

FIGURE 2: Expression of AQP5 protein in primary cultures of astrocytes of different ages. AQP5 protein was detected by Western blot analysis. The protein was detected in 1-, 2-, 3-, and 4-week-old primary cultures of astrocytes. β-Actin was used as internal control. The bottom panel is a quantification of the protein levels of AQP5 in primary cultures of astrocytes of different ages. $n = 4$ from three different experiments. *$P < 0.05$, **$P < 0.01$.

with the localizations of AQP5 and AQP4-EGFP in primary culture of astrocytes (Supp. Info. Fig. S2). In addition, the AQP4 and AQP5 immunostaining signals on the astrocyte cytoplasmic membranes did not co-localize (Fig. 4B). To confirm the distribution of AQP5 in astrocytes, we isolated the nuclear fraction and cytoplasmic fraction, which included the cytoplasm and cytoplasmic membrane, from astrocytes, and measured the expression of AQP5 in these fractions with Western blots (Fig. 4C). In primary cultures of astrocytes, there was only one detectable band for AQP5 (a little lower than the 26 kDa protein molecular weight marker) in the total cell lysate and cytoplasmic fraction, but no band in the nuclear fraction. β-Tubulin was only detected in the total cell lysate and cytoplasmic fraction of primary cultures of astrocytes, while Lamin A was only detected in the total cell lysate and nuclear fraction of primary cultures of astrocytes. These results were consistent with the observations of AQP5 immunostaining. To confirm the detailed distribution of AQP5 observed by immunostaining, we further isolated the cytoplasmic membrane, cytosolic, nuclear, and mitochondrial fractions from astrocytes and examined the expression of AQP5 with Western blots (Fig. 4D,E). AQP5 was only detected in the total cell lysate, cytoplasmic membrane, and cytosolic fractions, but could not be detected in the nuclear or mitochondrial fractions. β-Tubulin was only detected in the total cell lysate, cytoplasmic membrane, and cytoplasm fraction, Lamin A was only detected in the total cell lysate and nuclear fraction, the transferrin receptor (TfR) was mainly detected in the cytoplasmic membrane fraction, and COX4 was mainly localized in the mitochondrial fraction. The immunostaining and Western blot data confirmed that AQP5 was localized in both the cytoplasm and cytoplasmic membrane.

Expression of AQP5 in Rat Brain

To investigate the expression of AQP5 *in vivo*, the AQP5 expression in rat brain was also studied with immunostaining (Fig. 5A). The results showed that there were significant AQP5 signals in GFAP-positive astrocytes in rat cerebral cortical slices. In addition, AQP5 was also localized in GFAP-negative cells in rat cerebral cortical slices. Meanwhile, omitting the AQP5 primary antibody totally eliminated all the red fluorescence signals (Fig. 5B) in the immunostaining results.

Expression Changes of AQP5 in Astrocytes under Ischemia Treatment

Cytoplasmic membrane localization of AQP5 implicated that AQP5 could be involved in water movement across the membranes of astrocytes. We used real-time PCR to study the expression changes of AQP5 in astrocyte primary cultures under ischemia injury (Fig. 6A). The AQP5 mRNA expression was downregulated with ischemia treatment from 0.5 to 6 h. AQP5 mRNA expression significantly decreased by 40%–45% after ischemia treatment for 1 h, and its expression was decreased by 80% after ischemia treatment for 6 h. To investigate whether the protein expression of AQP5 also decreased with ischemia treatment, we studied the AQP5 protein expression in primary cultures of astrocytes under different lengths of ischemia treatment by Western blot (Fig. 6B). The AQP5 protein expression was also continually downregulated with ischemia treatment from 0.5 to 6 h. The AQP5 protein expression was significantly decreased by 40% after ischemia treatment for 2 h, and its expression decreased by 50% after ischemia treatment for 6 h. Thus, both the mRNA and protein expression of AQP5 were downregulated in primary cultures of astrocytes under ischemia treatment. The downregulation of AQP5 in primary cultures of astrocytes during ischemia treatment was also confirmed by immunostaining (Fig. 6C). Laser confocal microscopy revealed that the AQP5 signals were downregulated by ischemia injury, and they were localized on the cytoplasmic membrane and cytoplasm.

We have compared the expression changes of AQP1, 4, and 5 in astrocytes under ischemia treatment with Western blot (Supp. Info. Fig. S3). The results revealed that AQP5 was downregulated under ischemia treatment, AQP4 was upregulated under ischemia treatment, and there was no

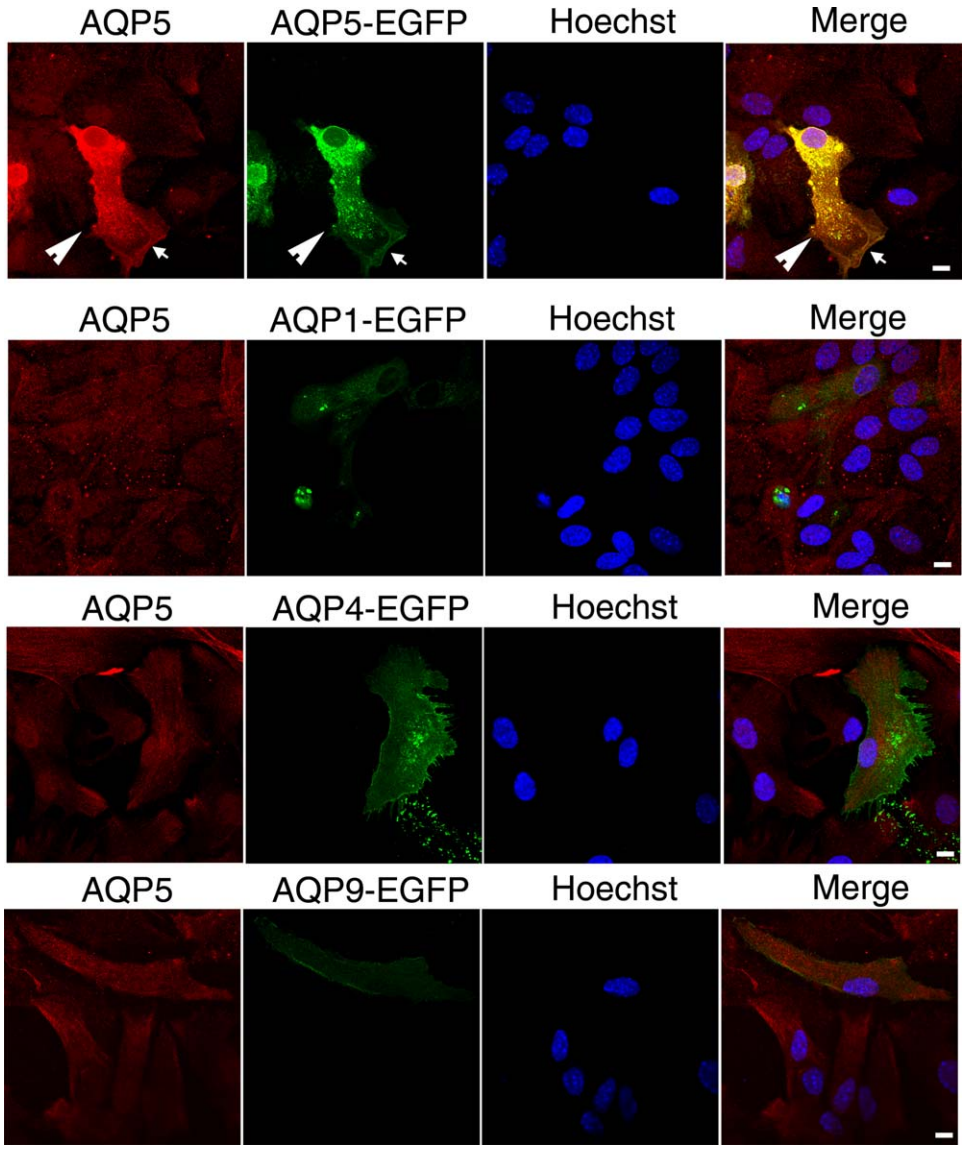

FIGURE 3: Specificity of AQP5 antibody and localization of AQP-EGFPs in primary cultures of astrocytes. AQP5 immunostaining was performed with astrocytes transfected with AQP-EGFPs (AQP1, 4, 5, and 9-EGFP), and observed with a laser confocal microscope. AQP5 immunostaining signals were shown in red, and other AQP-EGFP signals were shown in green. Increased AQP5 immunostaining signals were co-localized with AQP5-EGFP signals in AQP5-EGFP positive astrocytes (white arrowheads), and cytoplasmic membrane localization of both AQP5 immunostaining and AQP5-EGFP signals were identified with white arrows. Bar = 10 μm. All the pictures shown in the figure were representative pictures from at least three cultures from at least two independent experiments. [Color figure can be viewed in the online issue, which is available at wileyonlinelibrary.com.]

significant change in AQP1 expression. The quantitative results confirmed the relatively stable expression of AQP1 in astrocytes under ischemia treatment (Supp. Info. Fig. S3B). These findings indicated that AQP5 was regulated differently from other AQPs under ischemia treatment.

Expression of AQP5 was Downregulated in MCAO

The MCAO model was used to study AQP5 expression during brain injury *in vivo*. The expression changes of AQP5 in the cerebral cortex of rats during ischemia and reperfusion injury caused by MCAO was investigated with immunostaining (Fig. 7A,B). AQP5 was downregulated in the infarction in the cerebral cortex of rats after 2 h of ischemia treatment caused by MCAO, and its expression was continually downregulated during the reperfusion from 0 to 24 h both in GFAP-positive astrocytes and other GFAP-negative cells. Changes in the percentage of AQP5-positive cells in GFAP-positive cells were also analyzed. The percentage of AQP5-positive astrocytes decreased significantly after ischemia and reperfusion injury caused by MACO, dropping from 75% in uninjured brain to 10% in the infarct area (Fig. 7C). The percentage of AQP5-positive astrocytes did not change in the

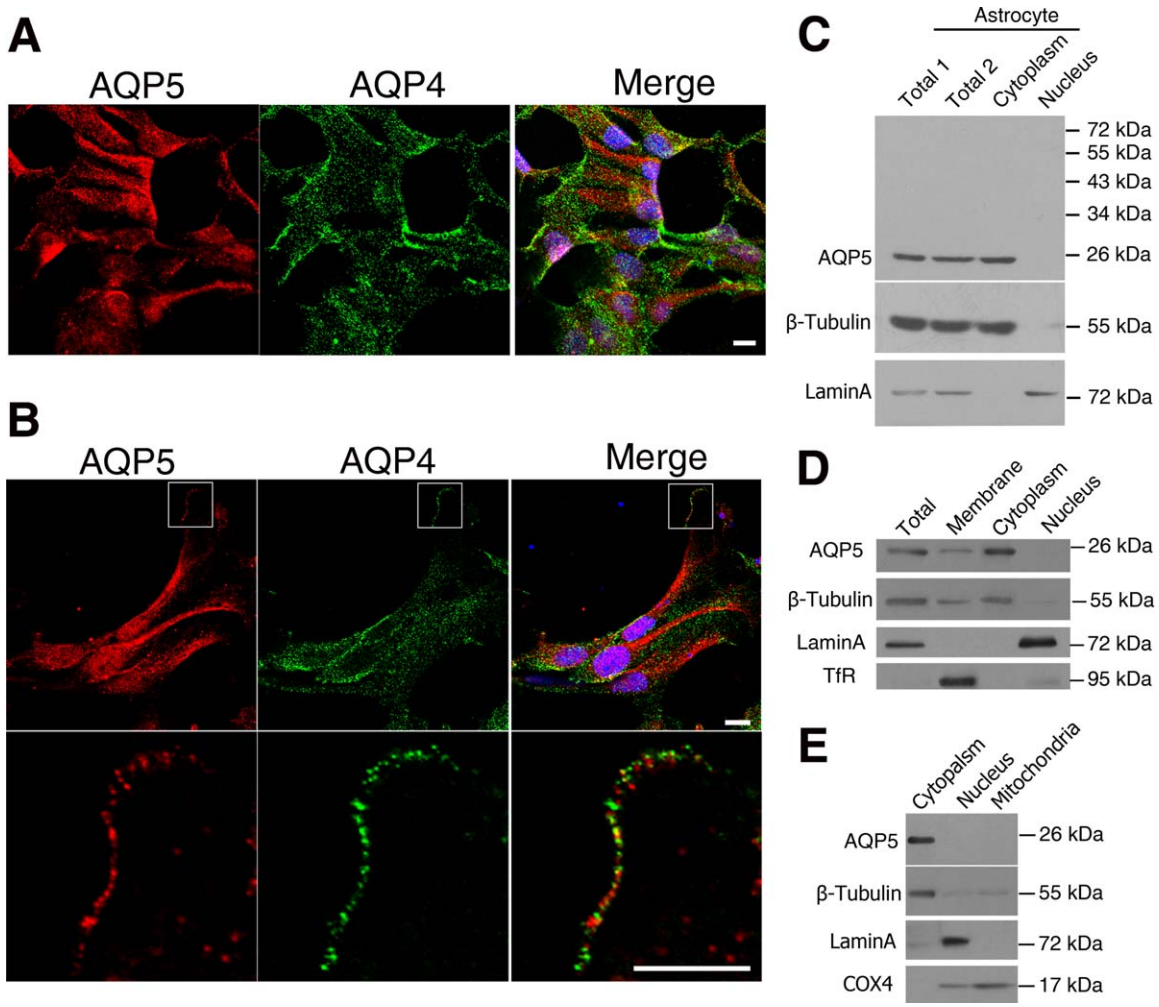

FIGURE 4: Localization of AQP5 in primary cultures of astrocytes. (A,B) Double immunostaining was performed with AQP5 and AQP4 primary antibodies in primary cultures of astrocytes. AQP5 was labeled red, AQP4 was labeled green, and nuclei were identified by Hoechst (blue). (B) Higher magnifications of the area shown in the white boxes from the upper panels were shown in the lower panels. Bar = 10 μm. (C–E) Expression and distribution (Western blots) of AQP5 in astrocytes in primary culture. (C) β-Tubulin and Lamin A were used as controls. Total 1, Total 2, total cell lysates from two cultures; Cytoplasm, cytoplasmic fraction including the cytoplasmic membrane; Nucleus, nuclear fraction. (D,E) β-Tubulin, Lamin A, transferrin receptor (TfR), and COX4 were used as controls. Total, total cell lysate; Membrane, cytoplasmic membrane fraction; Cytoplasm, cytoplasmic fraction; Nucleus, nuclear fraction; Mitochondria, mitochondrial fraction. All the pictures were representative pictures from at least three different cultures. [Color figure can be viewed in the online issue, which is available at wileyonlinelibrary.com.]

penumbra area (Fig. 7D). The AQP5 fluorescence intensity was also significantly decreased in the infarct area during injury (Fig. 7E) and did not change in the penumbra area (Fig. 7F). These results confirmed that AQP5 expression was downregulated during ischemia injury *in vivo*.

Expression of AQP5 was Upregulated in Astrocytes after Scratch-Wound Injury

We investigated the expression changes of AQP5 during traumatic injury. The scratch-wound injury model in primary cultures of astrocytes was used to investigate the expression of AQP5 in astrocytes after traumatic injury. The AQP5 mRNA expression changes in primary cultures of astrocytes at different times after scratch-wound injury were examined by real-time PCR (Fig. 8A). AQP5 mRNA expression decreased non-significantly at 4 h after scratch injury, followed by a steady increase that became significant at 12 and 24 h. We examined the AQP5 protein expression in primary cultures of astrocytes at different times after scratch injury by Western blot (Fig. 8B). The AQP5 protein was significantly increased at 6 and 12 h after scratch injury. Thus, both the mRNA and protein expressions of AQP5 were upregulated in primary cultures of astrocytes after scratch injury. The expression and distribution of AQP5 in primary cultures of astrocytes during scratch injury was also investigated with immunostaining (Fig. 8C–E). Astrocytes at the margin of the scratch wound injury

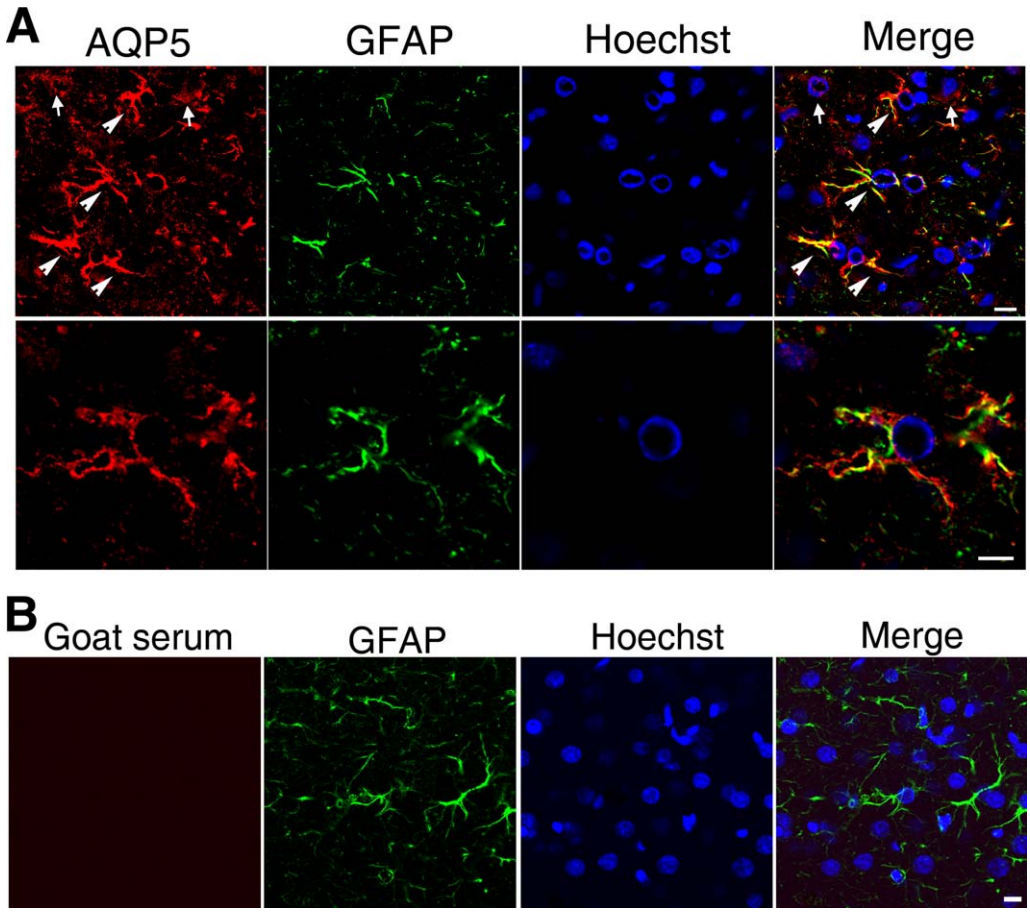

FIGURE 5: Expression of AQP5 in rat brain. Localization of AQP5 in cerebral cortex of rat brain was detected by immunostaining. The brain slice was observed with a laser confocal microscope. (A) AQP5 was labeled red, GFAP was labeled green, and nuclei were labeled with Hoechst (blue). AQP5 in GFAP-positive cells was indicated with white arrowheads, and AQP5 in GFAP-negative cells was indicated with white arrows. The lower panel showed the expression and localization of AQP5 in the GFAP-positive astrocyte with high magnification. Bar = 10 μm. All the pictures shown in the figure were representative pictures from at least three different slices. (B) Immunostaining was performed without AQP5 primary antibody (instead with goat serum) with normal rat brain slices. Bar = 10 μm. [Color figure can be viewed in the online issue, which is available at wileyonlinelibrary.com.]

became hypertrophic, and the astrocyte processes migrated into the wound 12 h after the scratch injury. The expression of AQP5 was significantly increased along the processes undergoing migration (Fig. 8C,D) but not in cells further away from the scratch wound (Fig. 8D). The expression of AQP5 in the processes undergoing migration into the scratch persisted for at least 48 h after scratch (Fig. 8E).

Overexpression of AQP5 Increased the Process Lengths of Reactive Astrocytes after Scratch-Wound Injury

Increased expression of AQP5, in the processes undergoing migration and the cytoplasmic membrane after scratch injury, indicated that AQP5 may play important roles in astrocyte process migration. To study the role of AQP5 in astrocyte migration after scratch injury, we compared the process lengths of astrocytes with or without AQP5 overexpression in the leading edge of scratch-wounds at 12, 24, and 36 h after scratch injury (Fig. 9A,B). The lengths of astrocyte processes in the leading edges of scratch-wounds increased with time after scratch injury, and the process lengths were significantly increased in AQP5-EGFP transfected astrocytes, but not in EGFP-N1 transfected astrocytes, compared with untransfected astrocytes. These results indicated that upregulation of AQP5 in astrocytes may be involved in cell migration after scratch injury.

AQP5 Expression was Increased in Reactive Astrocytes during In Vivo Stab-Wound Injury

To study the expression changes of AQP5 in astrocytes *in vivo* after traumatic injury, the AQP5 expression in rat cerebral cortex after stab-wound injury was examined with immunostaining (Fig. 10). The expression of AQP5 was significantly increased around the lesion site (Fig. 10A,B).

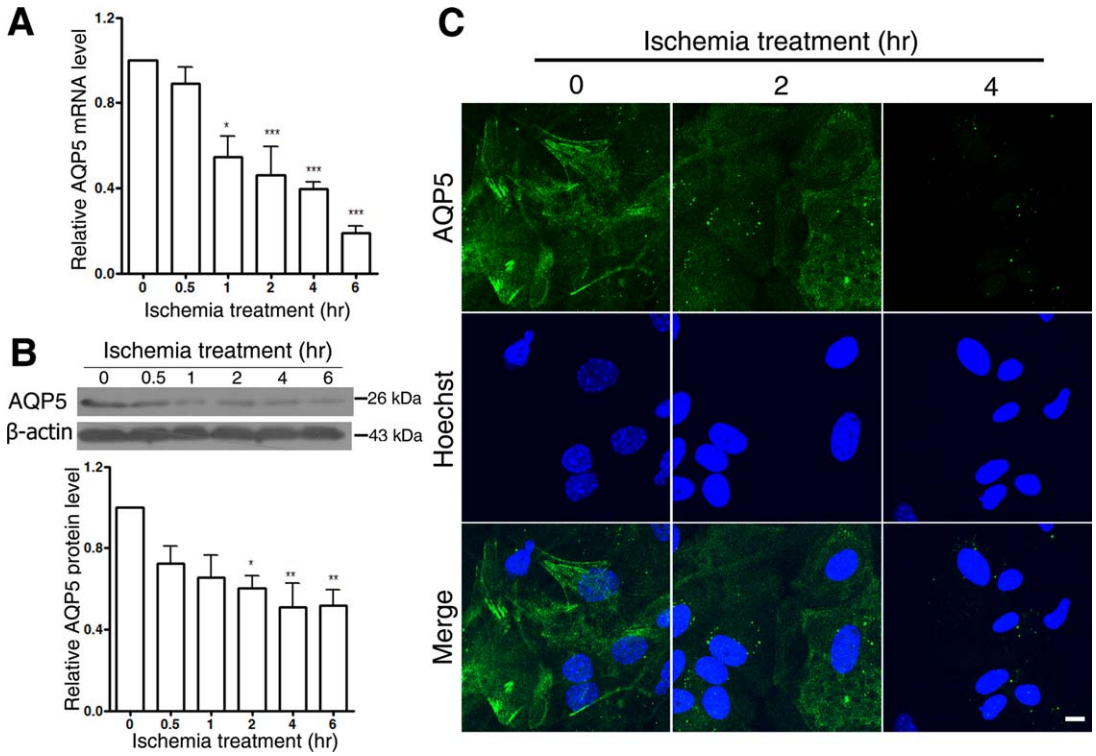

FIGURE 6: AQP5 expression in astrocytes with ischemia treatment. (A) The mRNA expression of AQP5 in primary cultures of astrocytes under 0–6 h of ischemia treatment was measured by real-time PCR. $n = 8$ from four different experiments. *$P < 0.05$, ***$P < 0.001$. (B) The protein expression of AQP5 in primary cultures of astrocytes under 0–6 h of ischemia treatment was measured by Western blot. β-Actin was used as internal control. The bottom panel is a quantification of the protein levels of AQP5 in primary cultures of astrocytes under 0–6 h of ischemia treatment. $n = 8$ from four different experiments. *$P < 0.05$, **$P < 0.01$. (C) The expression level of AQP5 in primary cultures of astrocytes under 0, 2, and 4 h of ischemia treatment was compared after immunostaining and observed with a laser confocal microscope. AQP5 was labeled green and nuclei were identified by Hoechst (blue). Bar = 10 μm. All the pictures shown were representative pictures from at least three different cultures. [Color figure can be viewed in the online issue, which is available at wileyonlinelibrary.com.]

The expression of GFAP was also significantly increased around the lesion site, and an increased AQP5 signal in both GFAP-positive astrocytes and GFAP-negative cells was observed. In addition, the change in the percentage of AQP5-positive cells in GFAP-positive cells in the glial scar caused by stab-wound injury was also analyzed. The percentage of AQP5-positive astrocytes increased significantly in the glial scar caused by stab-wound injury, increasing from 75% in un-injured brain to about 90% in the glial scar (Fig. 10C). To confirm that our observations from immunostaining were not caused by the unspecific binding of our red fluorescence-labeled secondary antibody, we also performed immunostaining without AQP5 primary antibody, and the results showed that there was no detectable red signal in the stab wound sites where GFAP increased expression was observed (Supp. Info. Fig. S4).

Discussion

Astrocytes exhibit the most prominent swelling during brain edema (Albertini and Bianchi, 2010; Badaut et al., 2002; Tait et al., 2008; Yang et al., 2011). AQPs in astrocytes therefore play a critical role in water homeostasis in the brain. Reports have suggested that the expression and distribution of different AQPs in astrocytes should be considered when determining the contribution of AQPs to brain water flux regulation (Albertini and Bianchi, 2010; Badaut et al., 2002; Liu and Wintour, 2005). In this study, we confirmed the expression of AQP4 and AQP5 in the cerebral cortex and astrocytes. We also detected both AQP4 and AQP5 in 1- to 4-week-old primary cultures of astrocytes. For this initial study of AQP5 protein expression in primary cultures of astrocytes and rat brain in normal, ischemia and traumatic injured conditions, we have carefully used a specific AQP5 antibody. This antibody has been used in previous studies and was shown to detect AQP5 without cross-reaction with other AQPs (Kumar et al., 2011; Moon et al., 2003; Zhang et al., 2008). We also performed experiments to re-confirm the specificity of the AQP5 antibody, and the results indicated that it specifically reacted with only AQP5, but not AQP1, 4, or 9. The important roles of AQP5 that have been reported (Krane et al.,

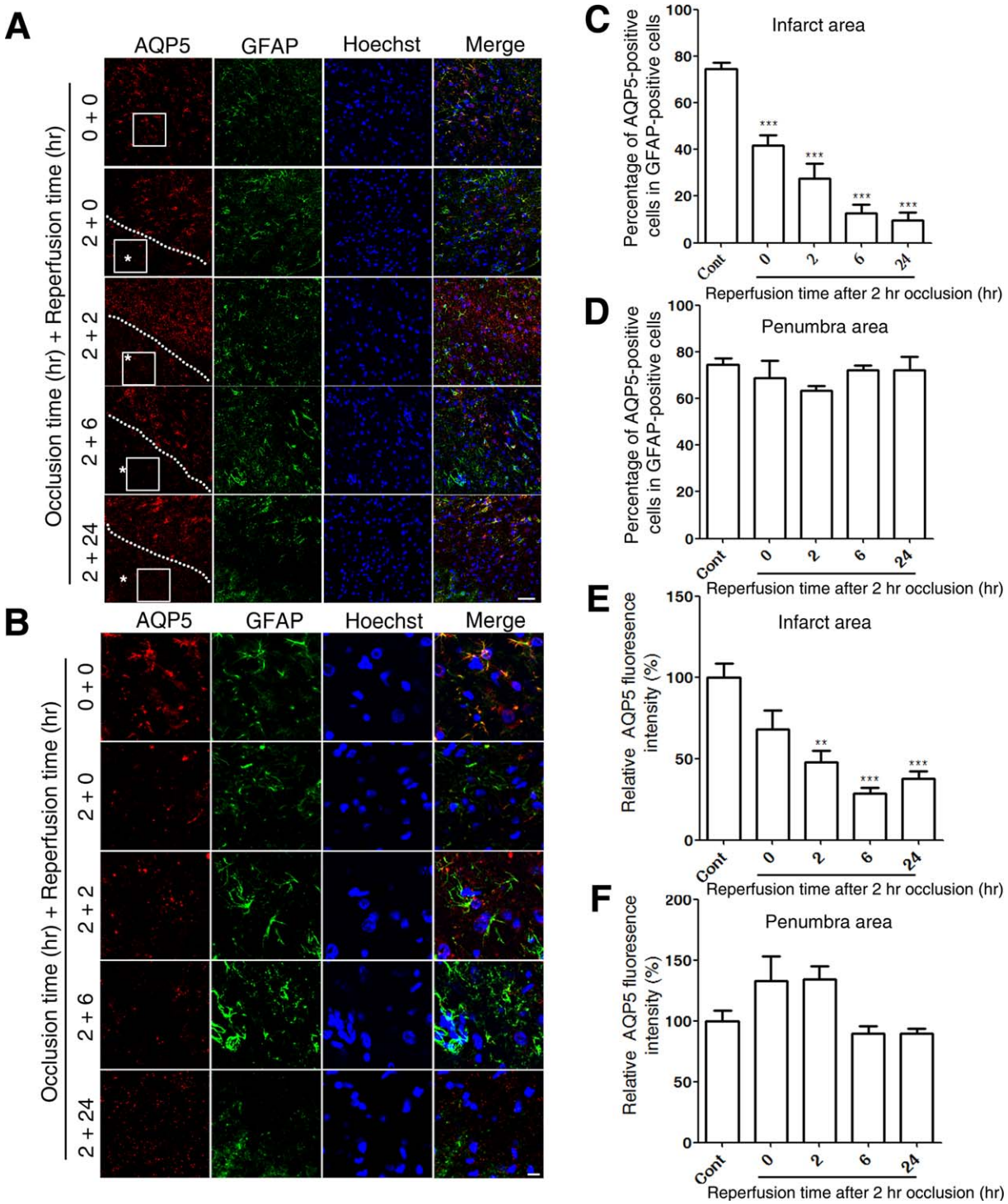

FIGURE 7: Expression of AQP5 in brains of rats with 2 h treatment of MCAO with different reperfusion times. **(A)** AQP5 expression levels in the infarct area (shown with a dotted line and white star) and surrounding areas of rat cerebral cortex with different reperfusion times after 2 h MCAO treatment were compared after immunostaining, and were observed with a laser confocal microscope. AQP5 was labeled red, GFAP was labeled green, and nuclei were identified with Hoechst (blue). Bar = 50 μm. **(B)** Higher magnifications of the regions shown in the white boxes from A. Bar = 10 μm. **(C,D)** Percentage of AQP5-positive cells in GFAP-positive cells in infarct areas **(C)** and penumbra areas **(D)** of rat cerebral cortex with different reperfusion times after 2 h MCAO treatment. ***$P < 0.001$, $n = 3–5$. **(E,F)** Relative AQP5 fluorescence intensity in infarct areas **(E)** and penumbra areas **(F)** of rat cerebral cortex with different reperfusion times after 2 h MCAO treatment. **$P < 0.01$, ***$P < 0.001$, $n = 3–5$. All the pictures were representative pictures from at least three different experiments. [Color figure can be viewed in the online issue, which is available at wileyonlinelibrary.com.]

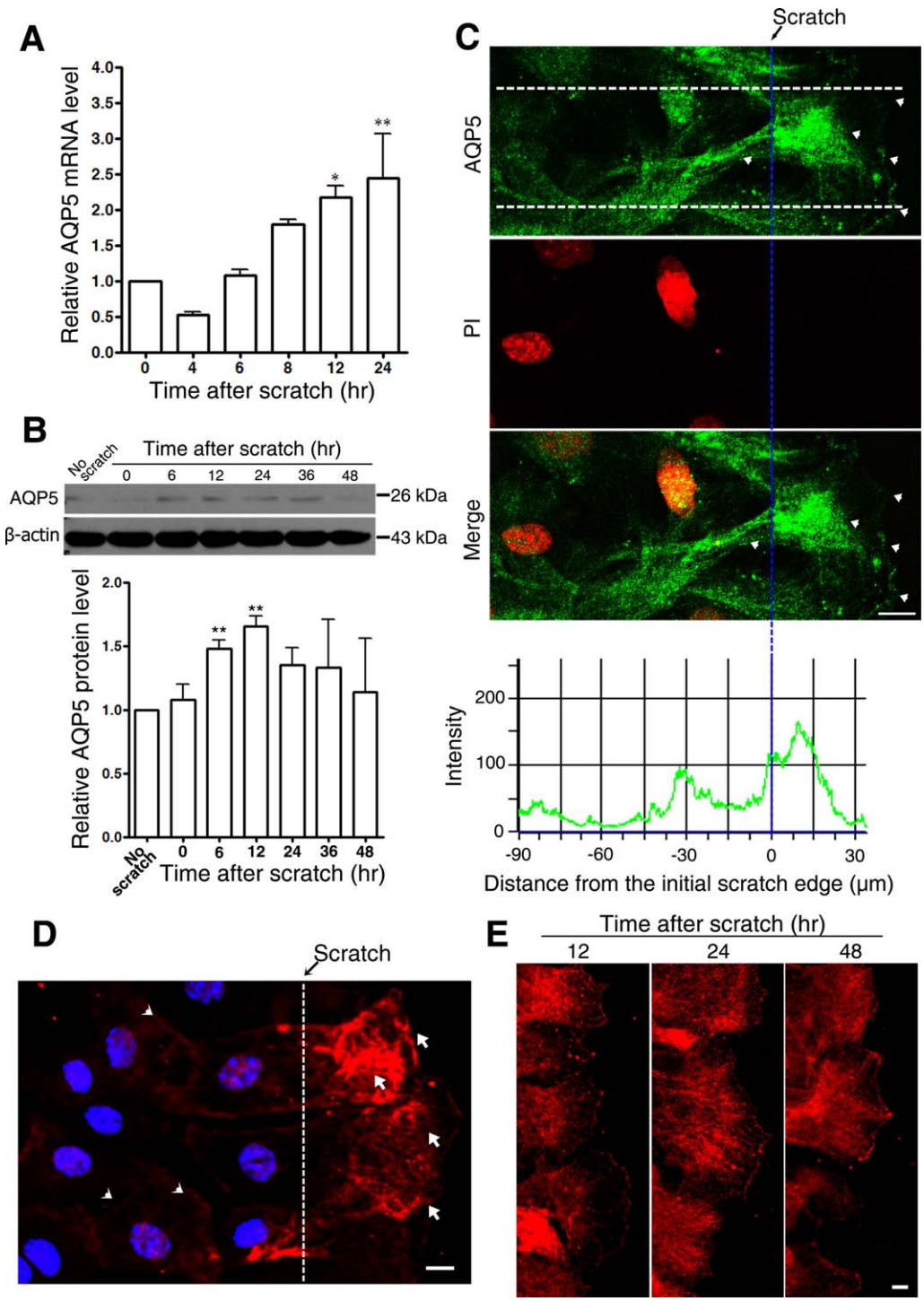

FIGURE 8: AQP5 expression in astrocytes after scratch. **(A)** Quantification of AQP5 mRNA expression in primary cultures of astrocytes after scratch injury was measured by real-time PCR. $n = 6$ from three different experiments. $^{*}P < 0.05$, $^{**}P < 0.01$. **(B)** The protein expression of AQP5 in primary cultures of astrocytes at 0–48 h after scratch injury was measured by Western blot. β-Actin was used as control. The bottom panel is a quantification of the protein levels of AQP5 in primary cultures of astrocytes at different times after scratch injury. $n = 6$ from three different experiments. $^{**}P < 0.01$. **(C)** Expression and distribution of AQP5 in astrocytes along the scratch-wound edge at 12 h after scratch injury was detected by immunostaining. AQP5 was labeled green (white arrowheads), nuclei were identified with PI (red), and the initial scratch injury edge was shown by the blue dotted line. The fluorescence intensity of AQP5 (the district between the two white dotted lines in the upper panel) at different distances from the initial scratch edge were shown in the lower panel. Bar = 10 μm. **(D)** The expression and localization of AQP5 (red, white arrows) in astrocytes at the leading edge of the scratch-wound and AQP5 (red, white arrowheads) in astrocytes far from the scratch-wound at 12 h after scratch was compared through immunostaining, and observed with a laser confocal microscope. Nuclei (blue) were stained with Hoechst 33342. Bar = 10 μm. **(E)** The expression and localization of AQP5 (red) in the migrating processes of astrocytes at 12, 24, and 48 h after scratch was compared through immunostaining and observed with a laser confocal microscope. Bar = 10 μm. All the pictures shown in the figure were representative pictures from at least three different cultures. [Color figure can be viewed in the online issue, which is available at wileyonlinelibrary.com.]

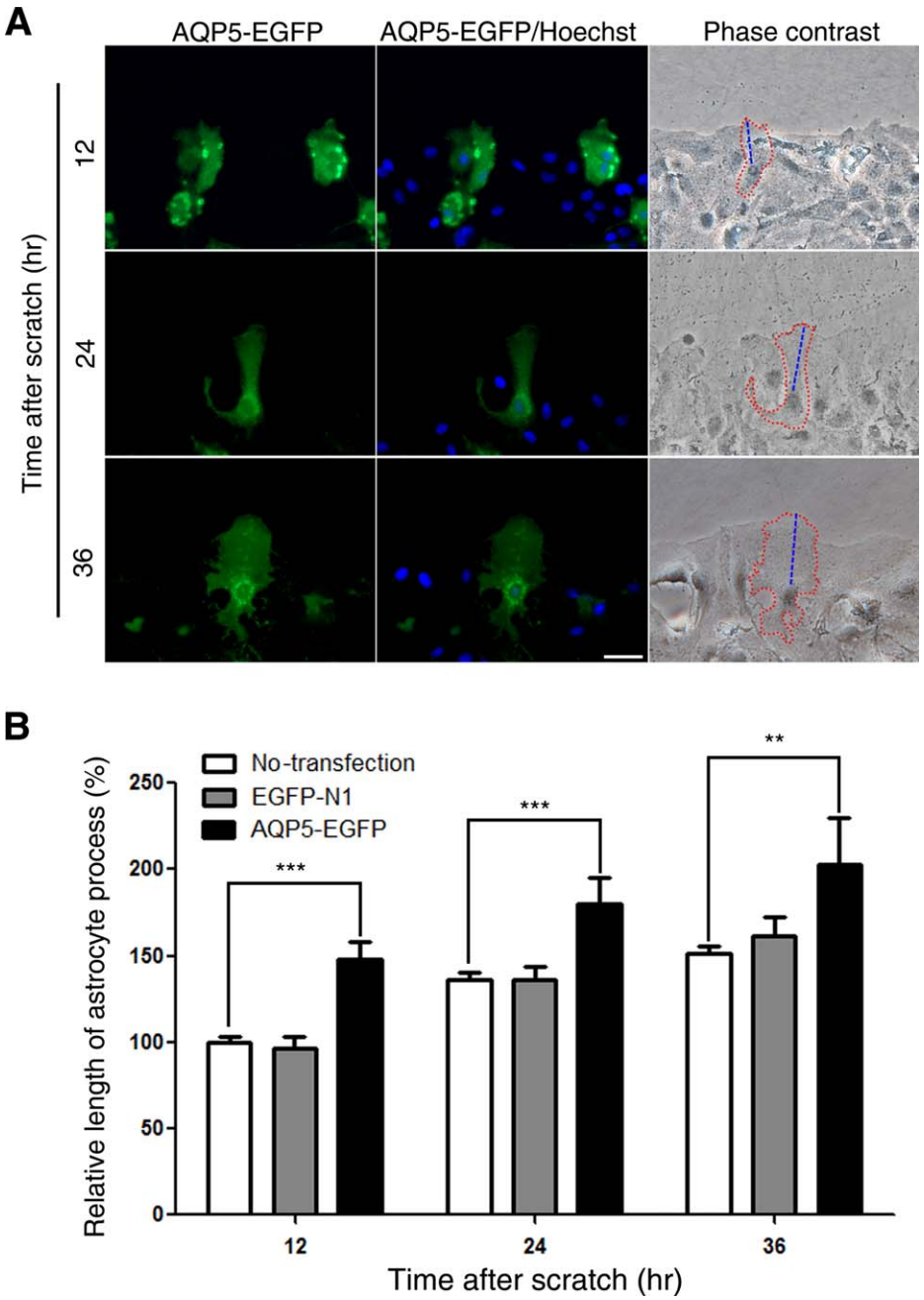

FIGURE 9: AQP5 overexpression facilitated astrocyte process growth after scratch injury. Primary cultures of astrocytes were scratched 12 h after AQP5-EGFP transfection and observed with a fluorescence microscope and a phase contrast microscope at 12, 24, and 36 h after scratch injury. (A) AQP5-EGFP (green) and nuclei (blue) were shown in fluorescence pictures. The processes of an astrocyte with (surrounded by a red dotted line) or without AQP5-EGFP overexpression at the leading edges of the scratch-wound were shown in phase contrast photographs. The lengths of the processes in astrocytes (from the nucleus to the leading edge of the process) were shown with blue dotted lines. Bar = 20 μm. (B) Quantification of the lengths of astrocyte processes at the leading edges of the scratch-wound at different times after scratch injury. For untransfected cells at least 100 cells were measured, for EGFP-N1 and AQP5-EGFP at least 20 cells were measured. **P < 0.01, ***P < 0.01. [Color figure can be viewed in the online issue, which is available at wileyonlinelibrary.com.]

2001; Ma et al., 1999; Sidhaye et al., 2006, 2012; Song and Verkman, 2001), taken together with our findings, indicate that AQP5 should also be considered when determining the functions of AQPs in astrocytes.

Different subcellular localizations of AQPs can indicate the different functions of these water channels. Previous studies showed that AQP4 is involved in astrocyte swelling (Fu et al., 2007; Gunnarson et al., 2008; Thrane et al., 2010)

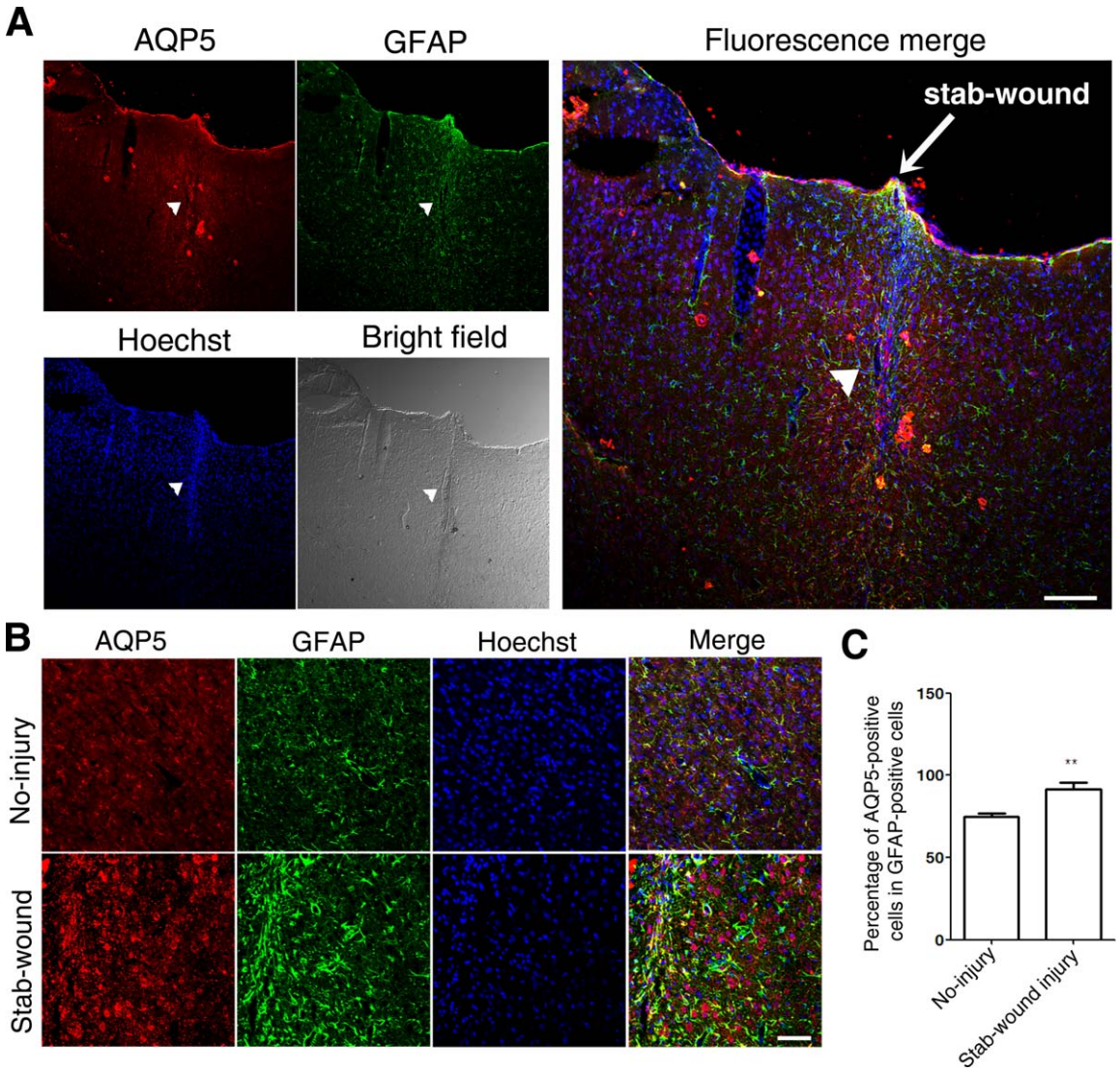

FIGURE 10: AQP5 expression in rat brain after stab-wound injury. The expression and distribution of AQP5 in rat cerebral cortex at 7 days after stab-wound injury was observed with a laser confocal microscope. AQP5 was labeled red, GFAP was labeled green, and nuclei were identified with Hoechst (blue). (A) The site of the stab-wound injury entry point was indicated with a white arrow, and glial scaring was indicated by white arrowheads. Bar = 200 μm. (B) AQP5, GFAP, and nuclei in the noninjury brain slice and stab-wound injury slice (7 days after stab wound injury). Bar = 100 μm. All the pictures shown in the figure were representative pictures from at least three slices. (C) Percentage of AQP5-positive cells in GFAP-positive cells in glial scar caused by stab-wound injury and noninjured cortex. **$P < 0.01$, $n = 5$. [Color figure can be viewed in the online issue, which is available at wileyonlinelibrary.com.]

and is also involved in K^+ flux as a result of its functional coupling with Kir 4.1 in the cytoplasmic membrane (Connors and Kofuji, 2006; Fort et al., 2008; Nagelhus et al., 1999). AQP3, localized on the cytoplasmic membrane, was reported to be involved in regulating signaling transduction (Miller et al., 2010). AQP8 and AQP9, localized in the mitochondrial membrane, participate in mitochondrial volume regulation and energy metabolism regulation (Amiry-Moghaddam et al., 2005; Calamita et al., 2005). AQP5 is involved in cytoplasmic membrane water permeability, paracellular water permeability, gas transduction, and transporting signaling molecules or coupling with other proteins in the membrane (Kawedia et al., 2007; Krane et al., 2001; Musa-Aziz et al., 2009; Sidhaye et al., 2006; Woo et al., 2008). In addition, AQP5 takes part in lung, breast, and colorectal cancer cell proliferation and migration (Jung et al., 2011; Wang et al., 2012; Zhang et al., 2010) and specifically interacts with microtubules to enhance their organization and stability in the cytoplasm (Sidhaye et al., 2012). Herein, we showed by co-staining in the same astrocytes, that AQP4 was mainly localized on the cytoplasmic membrane of astrocytes, which is consistent with the work of others (Rash et al., 1998; Saadoun et al., 2005; Thrane et al., 2010), while AQP5 was localized on both the cytoplasmic membrane and in the

cytoplasm of astrocytes, suggesting that AQP5 may be involved in multiple functions in astrocytes.

Brain ischemia is a frequent cause of brain edema, and ischemic injury results from a combination of substrate deprivation, severe hypoxia and failure to remove toxic metabolic products (Yu et al., 1995). AQPs play an important role in brain edema caused by ischemia injury. AQP4 is being considered as a potential target for brain ischemia treatment (Papadopoulos and Verkman, 2013; Zador et al., 2009). When it was knocked out in mice, the brain edema caused by focal ischemia during MCAO is reduced (Manley et al., 2000). In this study, we demonstrated that AQP5 expression was downregulated in primary cultures of astrocytes when treated with ischemia in our *in vitro* ischemia model. There has also been a report on AQP5 mRNA downregulation in rat astrocytes after hypoxia treatment (Yamamoto et al., 2001), which is consistent with our findings. Our study also indicated that AQP5 expression changes in astrocytes under ischemia treatment were different from the changes in AQP1 and AQP4. It is interesting to observe that AQP5 expression in astrocytes under ischemia injury was downregulated, while AQP4 was upregulated, both in this study and others (Nito et al., 2012; Qi et al., 2011; Tang et al., 2012). A similar downregulation of AQP5 was observed *in vivo*, as shown by the decreases in AQP5 immunostaining signals and the percentage of AQP5-positive astrocytes in the infarct areas after MCAO; these changes were not observed in the penumbra areas. This result also differs from AQP4, which was upregulated in astrocytes in the core and border of infarct areas (Meng et al., 2004; Ribeiro Mde et al., 2006). This difference in response to ischemia between AQP5 and 4 in astrocytes might have been caused by different intra-cellular mechanisms. HIF-1α and proteasomes have been indicated as the key molecular participators involved in the decreased expression of AQP5 during hypoxia injury in mouse lung epithelial cell line MLE-12 (Kawedia et al., 2013), while upregulation of MAPK signal pathways is reported to be responsible for the increase of AQP4 during ischemia injury (Nito et al., 2012; Qi et al., 2011). We also observed that AQP1 protein expression did not change during ischemia treatment, which is consistent with the stable expression of AQP1 in brain during ischemia treatment (Ribeiro Mde et al., 2006). These findings indicated that AQP5 may play different roles from AQP1 and AQP4 in astrocytes under ischemia. AQP5 has been shown to be involved in cell volume regulation, and a decrease in AQP5 affects the volume-sensing machinery of salivary acinar cells (Krane et al., 2001). AQP5 expression also dynamically responds to different pathological conditions and is involved in epithelial barrier function, membrane permeability, and water homeostasis in the respiratory epithelia (Sidhaye et al., 2006, 2008). Although the exact functions of AQP5 in astrocytes during ischemia injury still requires further investigation, our findings suggested that AQP5, together with AQP4, may possibly participate in the regulation of astrocyte volume during ischemia.

Brain trauma can cause edema, astrocyte activation, and the formation of glial scars, which can initially limit the extent of the injury, but may become an obstacle to subsequent neuronal regeneration (Lau and Yu, 2001; McCoy and Sontheimer, 2010; Saadoun et al., 2005; Serrano-Perez et al., 2011; Yang et al., 2012; Yu et al., 1993). AQPs play important roles in astrocytes after brain trauma injury. AQP1 expression is upregulated and plays a role in astrocyte swelling after such injury (McCoy and Sontheimer, 2010). Although AQP4 regulation in brain trauma injury is still controversial (Finnie et al., 2011; Ke et al., 2001; Kiening et al., 2002; Sun et al., 2003), it has been shown that AQP4 is polarized to the leading edge of migrating astrocytes to facilitate astrocyte migration and scar formation after scratch-wound injury and cerebral cortical stab-wound injury (Saadoun et al., 2005). Herein, we studied AQP5 expression using a scratch-wound injury model in primary cultures of astrocytes to simulate brain trauma injury (Lau and Yu, 2001; Yu et al., 1993). We demonstrated that AQP5 expression was upregulated after scratch-wound injury in primary cultures of astrocytes, which was confirmed in a cerebral cortical stab-wound injury in rat brain, indicating a potential role of AQP5 in astrocyte response to brain trauma injury. The AQP5 protein changes occurred before mRNA changes after scratch injury, which may have been caused by activation of translation before transcription, and the nonsignificant decrease in the expression of AQP5 mRNA at 4 h after scratch injury was also consistent with this conjecture. AQP5 is involved in cell proliferation and cell migration in cancer and has become a marker for cell proliferation and migration of breast cancer cells (Jung et al., 2011; Wang et al., 2012). AQP5 expression also facilitates tumor metastasis, and AQP5 has been detected in commonly used human glioma cell lines and acute patient biopsies (Jung et al., 2011; McCoy and Sontheimer, 2007; Shi et al., 2012; Wang et al., 2012; Zhang et al., 2010). Recently, the mechanisms behind brain tumorigenesis and reactive astrocyte migration in our scratch-wound injury model have been shown to be similar (Yang et al., 2012). Our findings here revealed that AQP5 was polarized to the leading processes of migrating astrocytes after scratch injury, and its expression was also increased in glial scars in stab-wound injured rat brain. In addition, overexpression of AQP5 increased the length of the migrating processes of astrocytes after scratch injury. These results indicated that AQP5 could possibly be involved in astrocyte activation and glial scar formation after traumatic brain injury. AQP5 abundance is associated with changes in actin organization, and

AQP5 directly and specifically interacts with microtubules to enhance microtubule organization and stability in primary human bronchial epithelial cells (Kawedia et al., 2007; Sidhaye et al., 2012). Cytoskeleton depolymerization and repolymerization are required for cell migration, and these processes have been shown to be the mechanism by which AQPs facilitate cell migration (Papadopoulos et al., 2008). Increased AQP5 in both the cytoplasm and cytoplasmic membrane of migrating processes of astrocytes after scratch could possibly participate in the astrocyte response to scratch injury, and may therefore be involved in facilitating astrocyte migration.

The differential regulation of AQP5 in astrocytes under ischemia injury and traumatic injury may be caused by different mechanisms under these two different injuries types (Lau and Yu, 2001). As mentioned before, ischemia injury may downregulate AQP5 through activating the HIF-1α signal pathway as reported during hypoxia injury (Kawedia et al., 2013). However, the mechanism behind AQP5 upregulation after traumatic injuries is still unclear, although traumatic injury activates p38 MAPK signal pathways, which have been reported to be involved in upregulating various AQPs, including AQP1, 4, 5, and 9 (Arima et al., 2003; McCoy and Sontheimer, 2010). p38 MAPK activation is also accompanied by AQP5 downregulation in A549 cells treated with transforming growth factor-β1 (Chen et al., 2013). Ischemia upregulates AQP4 expression through activation of MAPK signal pathways (Nito et al., 2012), but our results show that AQP5 was downregulated under ischemia. Therefore, the exact mechanism for the differential regulation of AQP5 in astrocytes under ischemia injury and traumatic injury will be an important topic for future studies and will also provide new evidence for understanding the mechanisms of the differential regulations of AQPs under different injuries.

In this study, we have examined AQP5 expression in astrocytes under normal, ischemic, and traumatic injury conditions in both mouse primary culture and rat animal models. There may be a potential variation in the expression of AQPs between mouse and rat, for example, AQP8 is expressed in mouse heart, but is not expressed in rat heart (Butler et al., 2006). Our data, however, confirmed that AQP5 was expressed in both mouse and rat astrocytes. We also demonstrated that AQP5 could be detected in mouse brain, mouse primary cultures of astrocytes, and astrocytes in rat brain tissues. Furthermore, the responses of AQP5 in rat brain astrocytes and mouse primary cultures were consistent under ischemic and traumatic injuries. Therefore, the expression and regulation of AQP5 in astrocytes of mouse and rat are potentially similar. We also observed AQP5 expression in cultured neurons and GFAP-negative cells in rat brain, and the level of AQP5 in GFAP-negative cells was decreased in MCAO injury but increased in stab-wound injury. AQP4 expression has been detected in activated microglia after stab-wound injury and is involved in immunological functions during glial scar formation (Ikeshima-Kataoka et al., 2013). AQP5 expression and function in neurons and microglia will therefore be an important topic for future studies.

In summary, this study has demonstrated that AQP5 was localized in the cytoplasm and on the cytoplasmic membrane of astrocytes, and its expression was increased during the development of astrocytes. AQP5 expression in astrocytes was downregulated during ischemia injury, but was upregulated after traumatic injury both *in vitro* and *in vivo*. We also showed that over-expression of AQP5 increased the process lengths of activated astrocytes after scratch injury. These findings indicated that AQP5 is a new addition to the important water channels in astrocytes, and revealed that AQP5 may participate in astrocyte responses to different injuries.

Acknowledgment

Grant sponsor: Beijing Natural Science Foundation; Grant number: 7091004; Grant sponsor: National Basic Research Program of China (973 program); Grant number: 2011CB504400; Grant sponsor: National Natural Science Foundation of China; Grant numbers: 30870818, 31070974, and 31171009; Grant sponsor: Foundation for Innovative Research Groups of the National Natural Science Foundation of China; Grant number: 81221002.

References

Agre P. 2006. The aquaporin water channels. Proc Am Thorac Soc 3:5–13.

Albertini R, Bianchi R. 2010. Aquaporins and glia. Curr Neuropharmacol 8: 84–91.

Amiry-Moghaddam M, Lindland H, Zelenin S, Roberg BA, Gundersen BB, Petersen P, Rinvik E, Torgner IA, Ottersen OP. 2005. Brain mitochondria contain aquaporin water channels: Evidence for the expression of a short AQP9 isoform in the inner mitochondrial membrane. FASEB J 19:1459–1467.

Anderova M, Antonova T, Petrik D, Neprasova H, Chvatal A, Sykova E. 2004. Voltage-dependent potassium currents in hypertrophied rat astrocytes after a cortical stab wound. Glia 48:311–326.

Arima H, Yamamoto N, Sobue K, Umenishi F, Tada T, Katsuya H, Asai K. 2003. Hyperosmolar mannitol simulates expression of aquaporins 4 and 9 through a p38 mitogen-activated protein kinase-dependent pathway in rat astrocytes. J Biol Chem 278:44525–44534.

Badaut J, Lasbennes F, Magistretti PJ, Regli L. 2002. Aquaporins in brain: Distribution, physiology, and pathophysiology. J Cereb Blood Flow Metab 22:367–378.

Badaut J, Regli L. 2004. Distribution and possible roles of aquaporin 9 in the brain. Neuroscience 129:971–981.

Bondy C, Chin E, Smith BL, Preston GM, Agre P. 1993. Developmental gene expression and tissue distribution of the CHIP28 water-channel protein. Proc Natl Acad Sci USA 90:4500–4504.

Butler TL, Au CG, Yang B, Egan JR, Tan YM, Hardeman EC, North KN, Verkman AS, Winlaw DS. 2006. Cardiac aquaporin expression in humans, rats, and mice. Am J Physiol Heart Circ Physiol 291:H705–H713.

Calamita G, Ferri D, Gena P, Liquori GE, Cavalier A, Thomas D, Svelto M. 2005. The inner mitochondrial membrane has aquaporin-8 water channels and is highly permeable to water. J Biol Chem 280:17149–17153.

Chen HH, Zhou XL, Shi YL, Yang J. 2013. Roles of p38 MAPK and JNK in TGF-beta1-induced human alveolar epithelial to mesenchymal transition. Arch Med Res 44:93–98.

Chen XQ, Qin LY, Zhang CG, Yang LT, Gao Z, Liu S, Lau LT, Fung YW, Greenberg DA, Yu AC. 2005. Presence of neuroglobin in cultured astrocytes. Glia 50:182–186.

Connors NC, Kofuji P. 2006. Potassium channel Kir4.1 macromolecular complex in retinal glial cells. Glia 53:124–131.

Dong Y, Liu HD, Zhao R, Yang CZ, Chen XQ, Wang XH, Lau LT, Chen J, Yu AC. 2009. Ischemia activates JNK/c-Jun/AP-1 pathway to up-regulate 14-3-3gamma in astrocyte. J Neurochem 109(Suppl 1):182–188.

Finnie JW, Blumbergs PC, Manavis J. 2011. Aquaporin-4 expression after experimental contusional injury in an ovine impact-acceleration head injury model. J Clin Neurosci 18:947–950.

Fort PE, Sene A, Pannicke T, Roux MJ, Forster V, Mornet D, Nudel U, Yaffe D, Reichenbach A, Sahel JA, Rendon A. 2008. Kir4.1 and AQP4 associate with Dp71- and utrophin-DAPs complexes in specific and defined microdomains of Muller retinal glial cell membrane. Glia 56:597–610.

Fu X, Li Q, Feng Z, Mu D. 2007. The roles of aquaporin-4 in brain edema following neonatal hypoxia ischemia and reoxygenation in a cultured rat astrocyte model. Glia 55:935–941.

Gunnarson E, Zelenina M, Axehult G, Song Y, Bondar A, Krieger P, Brismar H, Zelenin S, Aperia A. 2008. Identification of a molecular target for glutamate regulation of astrocyte water permeability. Glia 56:587–596.

Guo JJ, Liu F, Sun X, Huang JJ, Xu M, Sun FY. 2012. Bcl-2 enhances the formation of newborn striatal long-projection neurons in adult rat brain after a transient ischemic stroke. Neurosci Bull 28:669–679.

Hu Q, Ma Q, Zhan Y, He Z, Tang J, Zhou C, Zhang J. 2011. Isoflurane enhanced hemorrhagic transformation by impairing antioxidant enzymes in hyperglycemic rats with middle cerebral artery occlusion. Stroke 42:1750–1756.

Ikeshima-Kataoka H, Abe Y, Abe T, Yasui M. 2013. Immunological function of aquaporin-4 in stab-wounded mouse brain in concert with a pro-inflammatory cytokine inducer, osteopontin. Mol Cell Neurosci 56C:65–75.

Jung HJ, Park JY, Jeon HS, Kwon TH. 2011. Aquaporin-5: A marker protein for proliferation and migration of human breast cancer cells. PLoS One 6:1.

Kawedia JD, Nieman ML, Boivin GP, Melvin JE, Kikuchi K, Hand AR, Lorenz JN, Menon AG. 2007. Interaction between transcellular and paracellular water transport pathways through aquaporin 5 and the tight junction complex. Proc Natl Acad Sci USA 104:3621–3626.

Kawedia JD, Yang F, Sartor MA, Gozal D, Czyzyk-Krzeska M, Menon AG. 2013. Hypoxia and hypoxia mimetics decrease aquaporin 5 (AQP5) expression through both hypoxia inducible factor-1 alpha and proteasome-mediated pathways. PLoS One 8:e57541.

Ke C, Poon WS, Ng HK, Pang JC, Chan Y. 2001. Heterogeneous responses of aquaporin-4 in oedema formation in a replicated severe traumatic brain injury model in rats. Neurosci Lett 301:21–24.

Kiening KL, van Landeghem FK, Schreiber S, Thomale UW, von Deimling A, Unterberg AW, Stover JF. 2002. Decreased hemispheric aquaporin-4 is linked to evolving brain edema following controlled cortical impact injury in rats. Neurosci Lett 324:105–108.

King LS, Kozono D, Agre P. 2004. From structure to disease: The evolving tale of aquaporin biology. Nat Rev Mol Cell Biol 5:687–698.

Koyama Y, Takemura M, Fujiki K, Ishikawa N, Shigenaga Y, Baba A. 1999. BQ788, an endothelin ET(B) receptor antagonist, attenuates stab wound injury-induced reactive astrocytes in rat brain. Glia 26:268–271.

Krane CM, Melvin JE, Nguyen HV, Richardson L, Towne JE, Doetschman T, Menon AG. 2001. Salivary acinar cells from aquaporin 5-deficient mice have decreased membrane water permeability and altered cell volume regulation. J Biol Chem 276:23413–23420.

Kumar PA, Hu Y, Yamamoto Y, Hoe NB, Wei TS, Mu D, Sun Y, Joo LS, Dagher R, Zielonka EM, et al. 2011. Distal airway stem cells yield alveoli in vitro and during lung regeneration following H1N1 influenza infection. Cell 147:525–538.

Lau LT, Yu AC. 2001. Astrocytes produce and release interleukin-1, interleukin-6, tumor necrosis factor alpha and interferon-gamma following traumatic and metabolic injury. J Neurotrauma 18:351–359.

Liu H, Wintour EM. 2005. Aquaporins in development—A review. Reprod Biol Endocrinol 3:18.

Ma T, Song Y, Gillespie A, Carlson EJ, Epstein CJ, Verkman AS. 1999. Defective secretion of saliva in transgenic mice lacking aquaporin-5 water channels. J Biol Chem 274:20071–20074.

Manley GT, Fujimura M, Ma T, Noshita N, Filiz F, Bollen AW, Chan P, Verkman AS. 2000. Aquaporin-4 deletion in mice reduces brain edema after acute water intoxication and ischemic stroke. Nat Med 6:159–163.

McCoy E, Sontheimer H. 2007. Expression and function of water channels (aquaporins) in migrating malignant astrocytes. Glia 55:1034–1043.

McCoy E, Sontheimer H. 2010. MAPK induces AQP1 expression in astrocytes following injury. Glia 58:209–217.

Meng S, Qiao M, Lin L, Del Bigio MR, Tomanek B, Tuor UI. 2004. Correspondence of AQP4 expression and hypoxic-ischaemic brain oedema monitored by magnetic resonance imaging in the immature and juvenile rat. Eur J Neurosci 19:2261–2269.

Miller EW, Dickinson BC, Chang CJ. 2010. Aquaporin-3 mediates hydrogen peroxide uptake to regulate downstream intracellular signaling. Proc Natl Acad Sci USA 107:15681–15686.

Moon C, Soria JC, Jang SJ, Lee J, Obaidul Hoque M, Sibony M, Trink B, Chang YS, Sidransky D, Mao L. 2003. Involvement of aquaporins in colorectal carcinogenesis. Oncogene 22:6699–6703.

Musa-Aziz R, Chen LM, Pelletier MF, Boron WF. 2009. Relative CO_2/NH_3 selectivities of AQP1, AQP4, AQP5, AmtB, and RhAG. Proc Natl Acad Sci USA 106:5406–5411.

Nagelhus EA, Horio Y, Inanobe A, Fujita A, Haug FM, Nielsen S, Kurachi Y, Ottersen OP. 1999. Immunogold evidence suggests that coupling of K+ siphoning and water transport in rat retinal Muller cells is mediated by a coenrichment of Kir4.1 and AQP4 in specific membrane domains. Glia 26:47–54.

Nito C, Kamada H, Endo H, Narasimhan P, Lee YS, Chan PH. 2012. Involvement of mitogen-activated protein kinase pathways in expression of the water channel protein aquaporin-4 after ischemia in rat cortical astrocytes. J Neurotrauma 29:2404–2412.

Papadopoulos MC, Manley GT, Krishna S, Verkman AS. 2004. Aquaporin-4 facilitates reabsorption of excess fluid in vasogenic brain edema. FASEB J 18: 1291–1293.

Papadopoulos MC, Saadoun S, Verkman AS. 2008. Aquaporins and cell migration. Pflugers Arch 456:693–700.

Papadopoulos MC, Verkman AS. 2013. Aquaporin water channels in the nervous system. Nat Rev Neurosci 14:265–277.

Preston GM, Agre P. 1991. Isolation of the cDNA for erythrocyte integral membrane protein of 28 kilodaltons: Member of an ancient channel family. Proc Natl Acad Sci USA 88:11110–11114.

Preston GM, Carroll TP, Guggino WB, Agre P. 1992. Appearance of water channels in Xenopus oocytes expressing red cell CHIP28 protein. Science 256:385–387.

Qi LL, Fang SH, Shi WZ, Huang XQ, Zhang XY, Lu YB, Zhang WP, Wei EQ. 2011. CysLT2 receptor-mediated AQP4 up-regulation is involved in ischemic-like injury through activation of ERK and p38 MAPK in rat astrocytes. Life Sci 88:50–56.

Rash JE, Yasumura T, Hudson CS, Agre P, Nielsen S. 1998. Direct immunogold labeling of aquaporin-4 in square arrays of astrocyte and ependymocyte plasma membranes in rat brain and spinal cord. Proc Natl Acad Sci USA 95: 11981–11986.

Ribeiro Mde C, Hirt L, Bogousslavsky J, Regli L, Badaut J. 2006. Time course of aquaporin expression after transient focal cerebral ischemia in mice. J Neurosci Res 83:1231–1240.

Saadoun S, Papadopoulos MC, Watanabe H, Yan D, Manley GT, Verkman AS. 2005. Involvement of aquaporin-4 in astroglial cell migration and glial scar formation. J Cell Sci 118:5691–5698.

Serrano-Perez MC, Martin ED, Vaquero CF, Azcoitia I, Calvo S, Cano E, Tranque P. 2011. Response of transcription factor NFATc3 to excitotoxic and traumatic brain insults: Identification of a subpopulation of reactive astrocytes. Glia 59:94–107.

Shi WZ, Zhao CZ, Zhao B, Shi QJ, Zhang LH, Wang YF, Fang SH, Lu YB, Zhang WP, Wei EQ. 2012. Aggravated inflammation and increased expression of cysteinyl leukotriene receptors in the brain after focal cerebral ischemia in AQP4-deficient mice. Neurosci Bull 28:680–692.

Sidhaye VK, Chau E, Srivastava V, Sirimalle S, Balabhadrapatruni C, Aggarwal NR, D'Alessio FR, Robinson DN, King LS. 2012. A novel role for aquaporin-5 in enhancing microtubule organization and stability. PLoS One 7:8.

Sidhaye VK, Guler AD, Schweitzer KS, D'Alessio F, Caterina MJ, King LS. 2006. Transient receptor potential vanilloid 4 regulates aquaporin-5 abundance under hypotonic conditions. Proc Natl Acad Sci USA 103:4747–4752.

Sidhaye VK, Schweitzer KS, Caterina MJ, Shimoda L, King LS. 2008. Shear stress regulates aquaporin-5 and airway epithelial barrier function. Proc Natl Acad Sci USA 105:3345–3350.

Simon C, Gotz M, Dimou L. 2011. Progenitors in the adult cerebral cortex: Cell cycle properties and regulation by physiological stimuli and injury. Glia 59:869–881.

Song Y, Verkman AS. 2001. Aquaporin-5 dependent fluid secretion in airway submucosal glands. J Biol Chem 276:41288–41292.

Strange K. 1992. Regulation of solute and water balance and cell volume in the central nervous system. J Am Soc Nephrol 3:12–27.

Sun MC, Honey CR, Berk C, Wong NL, Tsui JK. 2003. Regulation of aquaporin-4 in a traumatic brain injury model in rats. J Neurosurg 98:565–569.

Tait MJ, Saadoun S, Bell BA, Papadopoulos MC. 2008. Water movements in the brain: Role of aquaporins. Trends Neurosci 31:37–43.

Tang Z, Liao Z, Xie Y, Shi Q, He C, Zhan Y. 2012. [Role of P38 signaling pathway in neonatal rat astrocyte swelling and aquaporin-4 expression after oxygen-glucose deprivation and recovery]. Nan Fang Yi Ke Da Xue Xue Bao 32:141–145.

Thrane AS, Rappold PM, Fujita T, Torres A, Bekar LK, Takano T, Peng W, Wang F, Thrane VR, Enger R, Haj-Yasein NN, Skare Ø, Holen T, Klungland A, Ottersen OP, Nedergaard M, Nagelhus EA. 2010. Critical role of aquaporin-4 (AQP4) in astrocytic Ca2+ signaling events elicited by cerebral edema. Proc Natl Acad Sci USA 108:846–851.

Wang W, Li Q, Yang T, Bai G, Li D, Sun H. 2012. Expression of AQP5 and AQP8 in human colorectal carcinoma and their clinical significance. World J Surg Oncol 10:1477–7819.

Woo J, Lee J, Kim MS, Jang SJ, Sidransky D, Moon C. 2008. The effect of aquaporin 5 overexpression on the Ras signaling pathway. Biochem Biophys Res Commun 367:291–298.

Yamamoto N, Yoneda K, Asai K, Sobue K, Tada T, Fujita Y, Katsuya H, Fujita M, Aihara N, Mase M, Yamada K, Miura Y, Kato T. 2001. Alterations in the expression of the AQP family in cultured rat astrocytes during hypoxia and reoxygenation. Brain Res Mol Brain Res 90:26–38.

Yang C, Iyer RR, Yu AC, Yong RL, Park DM, Weil RJ, Ikejiri B, Brady RO, Lonser RR, Zhuang Z. 2012. beta-Catenin signaling initiates the activation of astrocytes and its dysregulation contributes to the pathogenesis of astrocytomas. Proc Natl Acad Sci USA 109:6963–6968.

Yang CZ, Li HL, Zhou Y, Chai RC, Zhao R, Dong Y, Xu ZY, Lau LT, Yingge Z, Teng J, Chen J, Yu AC. 2011. A new specialization in astrocytes: Glutamate- and ammonia-induced nuclear size changes. J Neurosci Res 89: 2041–2051.

Yool AJ. 2007. Aquaporins: Multiple roles in the central nervous system. Neuroscientist 13:470–485.

Yu AC, Lee YL, Eng LF. 1993. Astrogliosis in culture: I. The model and the effect of antisense oligonucleotides on glial fibrillary acidic protein synthesis. J Neurosci Res 34:295–303.

Yu AC, Lee YL, Fu WY, Eng LF. 1995. Gene expression in astrocytes during and after ischemia. Prog Brain Res 105:245–253.

Yu AC, Wong HK, Yung HW, Lau LT. 2001. Ischemia-induced apoptosis in primary cultures of astrocytes. Glia 35:121–130.

Zador Z, Stiver S, Wang V, Manley GT. 2009. Role of aquaporin-4 in cerebral edema and stroke. Handb Exp Pharmacol 190:159–170.

Zhang Q, Zhang J, Moe OW, Hsia CC. 2008. Synergistic upregulation of erythropoietin receptor (EPO-R) expression by sense and antisense EPO-R transcripts in the canine lung. Proc Natl Acad Sci USA 105:7612–7617.

Zhang Z, Chen Z, Song Y, Zhang P, Hu J, Bai C. 2010. Expression of aquaporin 5 increases proliferation and metastasis potential of lung cancer. J Pathol 221:210–220.

Zhou Y, Li HL, Zhao R, Yang LT, Dong Y, Yue X, Ma YY, Wang Z, Chen J, Cui CL, Yu AC. 2010. Astrocytes express *N*-methyl-D-aspartate receptor subunits in development, ischemia and post-ischemia. Neurochem Res 35: 2124–2134.